Int.J.Curr.Microbiol.App.Sci (2019) Special Issue-9: 331-352

International Journal of Current Microbiology and Applied Sciences
ISSN: 2319-7706 Special Issue-9 pp. 331-352
Journal homepage: http://www.ijcmas.com

Original Research Article

Diurnal Variation of Clouds Cover Area and Clouds Top Temperature over Tropical Cyclone in the North Indian Ocean Basins

Vikash Kumar Sharma[1*], Prabhat Kumar[2], Satya Prakash Ojha[3] and Sanjay Kumar Sharma[4]

[1]Centre for Oceans River, Atmosphere and Land Sciences, Indian Institute of Technology Kharagpur, West Bengal-721302, India
[2]SMS Agromet KVK, Araria, Bihar Agriculture University, Sabour-813210, India
[3]Space Application Centre, ISRO, Ahmedabad, Gujarat- 380058, India
[4]Department of Seed Science and Technology, Bihar Agriculture University, Sabour-813210, India
**Corresponding author*

Keywords

Cloud Cover Area, Cloud Top Temperature, North Indian Ocean

A B S T R A C T

The diurnal variation of the Cloud Cover Area (CCA) and Cloud Top Temperature (CTT) during Tropical Cyclone (TC) convective cloud systems in the North Indian Ocean (NIO) basins are studied using thermal infrared brightness temperature (TIR-BT) data from Indian satellites and best-track data from India meteorological department (IMD) during 2008-2016. The diurnal variation of CCA of deep cold, cold and warm clouds are opposite in phase and magnitude in the inner region of TCs. The cold clouds had minimum mean CTT during the morning while warm cloud had minimum CTT during afternoon. The out- of-phase relationship between cold and warm clouds can both lead to the radius-averaged TIR-BT having two minimum per day. At a given time during the day, time the mean CTT increases with increase in the radial distance from the TC centre. The TIR-BT limits are also found to increase with the mean increase in mean CCA at a given instant during the day. The different diurnal evolutions under different cloud conditions suggest TC convective cloud systems are best described in terms of both CCA and CTT. Maximum occurrence of cloud with deep cold cloud in the morning and maximum occurrence of cold cloud at the afternoon suggest that two different mechanisms involved in causing diurnal variations of CCA and CTT under these two types of TC cloud conditions.

Introduction

Tropical cyclone (TC) is rapidly rotating system characterized by a low pressure centre, a closed low level atmospheric circulation, strong winds, and a spiral arrangement of thunderstorms that produce heavy rain (Holton and Hakim, 2012). The horizontal extent of TC ranges from 100-1000 km while it extends through the depth of troposphere (10-12 km) in vertical. TCs have anti-clockwise rotating winds at surface in the Northern Hemisphere (NH) and clockwise rotating winds at surface in the Southern Hemisphere (SH). The air moving into the centre near about the ground, moves out of the centre in the opposite direction as it moves away from the ground, namely clockwise in the NH and anticlockwise in the SH. Atmospheric pressure in the centre of strong TC can be more than 50 millibar (mb) lower than the surrounding environmental pressure, but in extreme cases the pressure difference can reach upto 100 mb (Gray, 1975). TCs are associated with the devastation caused by high wind speed, heavy rain fall, storm surge, and floods which causes the huge loss of life and property (Anthes *et al.,* 2006; Gray *et al.,* 1992). However, cyclones have positive impacts too; they regulate the climate by redistributing the heat pole ward from equator. TCs are categorized based on the Estimated Maximum Sustained Surface Wind (EMSSW), suggested by the World Meteorological Organization (WMO). The primary source of energy of the TC is the release of latent heat supplied by condensation of water vapour into water droplet or rain. TCs form only in warm ocean waters having Sea Surface Temperature (SST) greater than 26.5◦C up to 50 meters depth (Emanuel, 1989), TCs can't form within 5◦ latitude because coriolis force is too small there to maintain the cyclonic rotation of low-pressure system (Harr *et al.*, 1996). Another requirement of TC formation is an atmosphere, which is potentially unstable to moist convection (Gray, 1998). The low level wind shear is also plays an important role in the TC formation, The TCs can't form in-situ without any initial incipient disturbance. A fully developed TC has a central cloud free region of clam winds, known as eye of the cyclone with diameter varying from 10 to 50 km (Frank, 1977). Cyclone eye is the region having lowest surface pressure and warmest temperature from the surroundings, the cyclone eye is a wall of dense convective clouds rising about 15 km into atmosphere that is called eye-wall (Fiorino and Elsberry, 1989). Eyewall is the area where highest surface winds and maximum intensity of rainfall occur, while there are no rains at the centre of cyclones eye. The intensity of rainfall decreases from the eye wall towards the outer portions of the cyclone. The surface pressure gradient and surface wind speed both increases gradually from centre of the cyclone towards outside. Convection in TCs is organized into long, narrow rain bands which are oriented in the same direction as the horizontal wind. These bands often extend up to 1000 km from the cyclone centre (Gray, 1981), and contain heavy rain and wind squalls. TCs could be viewed as a special type of mesoscale convective system, which continues to develop over a huge source of relative warmth and moisture (Palmn and Riehl, 1957). The three-dimensional wind held in a TC can be separated into two components namely primary circulation and secondary circulation, the secondary circulation is based on the carnot heat engine. The Carnot heat engine contains four phases (Chan and Williams, 1987). In meteorology, the diurnal variation of temperature is the variation between a high temperature and a low temperature that occur during the same day. The diurnal variation signatures of CCA and Precipitation are majorly produced by TC in the tropic and sub tropic region (Shu *et al.*, 2013; Dunion *et al.,* 2014; Bowman and Fowler, 2015). The diurnal variation of CCA and CTT is caused by the structure of TCs, TCs intensity and incoming solar radiations (Dunion *et al.*, 2014). At the local noon, the incoming solar radiation goes to peak which causes the diurnal convection cycle so heating of earth surface and planetary boundary layer makes a maximum convective precipitation at late afternoon (e.g. Janowiak *et al.*, 1994; Yang and Slingo; 2001). Yang and Slingo (2001) noticed that the maximum deep CCA occurs at the early morning where as during the afternoon or early evening maximum cloud cover area over the ocean is being observed. Some theories describe the major importance for the differential radiative heating between the surrounding cloud-free region and the cloudy regions (Gray and Jacobson, 1977). According to Gray theory, the deep cold cloud cover area is maximum at morning due to direct radiation convection effect and at afternoon there is a suppressed convection due to much absorbed solar radiation by the cloud tops, which in effect increases the instability and also promotes convection (Randall *et al.,* 1991; Yang and Slingo, 2001). The precipitation rate is maximum during morning is caused by number of mesoscale convective system, here the growth is favoured and the lifetimes are long at night (Nesbitt and Zipser, 2003). The diurnal variation of maxima and minima of TCs are identified by infrared (IR) satellite images. It can observe that diurnal cycle has specific features of some inconsistencies, specifically in the cycle phases. Using CTT below specific thresholds the diurnal variation of CCA of TC is studied (e.g. Browner *et al.,* 1977; Muramatsu, 1983; Strenka *et al.,* 1984). Only eight Atlantic TCs are been analysed and noticed that CCA is minimum at 0300 LST and minimum at 1700 LST by Browner *et al.,* (1977). Strenka *et al.,* (1984) observed during early morning the inner core region of CCA with very lower IR-BT reaches its maximum. Having fixed annular and average temperatures, the CTT of TCs along with diurnal variation in IR-BT evaluated. A significant diurnal oscillation in CTT is also observed by Strenka *et al.,* (1984) and in annular region large percentage of the variation is observed varying from the inner core to the TCs periphery (i.e., hundreds kilometres from the centre) with a notice of semidiurnal CTT cycles at TCs outer periphery. The main importance of this study Very cold clouds are closely associated with precipitating deep convective clouds, and precipitation in TCs is closely related to the release of latent heat and the development of the TC (e.g. Steranka *et al.,* 1986; Rao and MacArthur, 1994; Kieper and Jiang, 2012). Cyclone structure and intensity depends on the latent heat release and LHR depends on precipitation and in turn precipitation depends on the CCA, so diurnal variations under different cloud conditions could have important influences on the structure and intensity of TCs.

Due to the presence of cloud bearing different properties, the diurnal variation in the CCA and CTT in TCs are caused. Mainly four types of cloud occur in atmosphere. High clouds, Middle clouds, Low clouds and vertically developed clouds. The highest clouds in the atmosphere are cirrocumulus, cirrus, and cirrostratus. Cumulonimbus clouds can also grow to be very high. Mid-level clouds include altocumulus and altostratus. The lowest clouds in the atmosphere are stratus, cumulus, and stratocumulus. The cloud with vertical development in the atmosphere is cumulus and cumulonimbus. The TIR-BT is measured using satellite IR sensors, which provide indirect estimates of the properties of deep cold cloud, cold cloud and warm cloud but do not determine the interior properties of the clouds (e.g. Liu *et al.,* 1995; Sui *et al.,* 1997). The average temperature within a fixed radius includes diurnal signals from different types of cloud.

Materials and Methods

We have used data from satellite as well as cyclone Best-track data. The cyclone best-track data is obtained from IMD (2008-2015) and JTWC (2015-2016) (Chu *et al.,* 2002). In best-track data, the cyclone parameters were typically recorded at 0000, 0300, 0600, 0900, 1200, 1500, 1800 and 2100 UTC. Three-hourly measurements of the location of the TC centre, the intensity of the TC, and other important parameters were included in the best-track data. In this study we used 3-hourly observations best track data from the IMD and 6-hourly data from JTWC were linearly interpolated to 3-hourly observations. About 31 cyclones are studied, in which 21 cyclones were in Bay of Bengal and 10 cyclones are from ARB basins. Wu and Z. Ruan separated two types of cyclones (week and strong) on the basis of categories 1 and categories 2-5 over pacific ocean but in NIO basins case the cyclones of categories 2-5 are very less so we cannot conclude the diurnal variability of strong cyclone properly hence all the types of cyclones are considered as whole. We have used two satellite data namely Kalpana-1 and INSAT-3D. We used TIR-BT (equivalent to black-body temperature) data with a pixel size of 8x8 km^2 and 4x4 km^2) from the Meteorological Oceanographic Satellite Data Archival Centre (MOSDAC) by merging two satellite data namely Kalpana1 (10.5-12.5 mm) and INSAT-3D (10.5-11.95 mm) respectively. In Kalpana-1 we used K1VHR-L1B TIR (10.5-12.5 mm) channel data from 25th Oct. 2008 to 13th Oct 2013 during cyclone period over NIO basins. The TIR channel data is available half-hourly on mosdac website (www.mosdac.gov.in) but we used 3-hourly data and the resolution of this data is 8 km. Now in INSAT3D we used Imager data L1B product of TIR-2 channel (11.95mm) brightness temperature from 23th Nov 2013 to 13th Dec 2016 during cyclone period over NIO basins, TIR-2 channel data is also available half-hourly on mosdac website (www.mosdac.gov.in) but we used 3-hourly and the resolution of this data is 4 km. A total of 1127 three-hourly satellite images (from Kalpana-1 and INSAT3D) were collected for BoB cyclones and 428 three-hourly satellite images (from Kalpana-1 and INSAT- 3D) were collected for ARB cyclones. In previous studies using TIR-BT of 230-240 K, TIR-BT < 210 K , and TIRBT < 235 K are indicate the presence of convective clouds, deep convective cloud and high cloud respectively (e.g Yang and Slingo; Machado *et al.*, 2002; Tian *et al.*, 2004). In western pacic Chen and Houze (1997) are found TIR-BT < 208 K is a deep convective precipitating clouds. Wu and Z. Ruan categorized the cloud types in three category on the basis of TIR-BT, namely very cold deep convective clouds (TIR-BT < 208 K), cold high clouds (208 K < TIR-BT < 240 K) and low level clouds or clear sky (TIR-BT > 240 K). The analysis the previous studies we take three thresholds of TIR-BT namely deep cold clouds (TIR-BT < 210 K), cold clouds (210 K< TIR-BT < 240 K) and warm clouds (TIR-BT > 240 K). Our analysis is focused on the open ocean only during cyclone life cycle before land fall but satellite images including island less than 200 km from a cyclone centre were not excluded. The diurnal variation of CTT and CCA is analysed within 500 km region from the TC centre, because after 500 to 1000 km the variation is negligible (Part and Nelson, 2013). Further, the region within the 500 km radius (whole) is sub-divided into two regions namely, inner (0-200 km) and outer (300-500 km) region and we also select different-different radius (e.g. 50, 100, 150, 200, 250, 300, 350, 400, 450, 500 km) from the TC centre. The CCA is defined as the area of the cyclone region covered by the cloudy pixels. We calculated total CCA over the cyclonic region (or over the specific annular region) by computing the area of the cloudy pixels. For the sake of simplicity in calculating the pixel area, the pixel is assumed to be a trapezoid. For calculating percentage of cloud covered area having TIR-BT with specific thresholds (within 500 km), Cloud Cover Area Percentage (CCAP), is defined as

$$CCAP_{BT<210\,K} = \frac{CCA_{BT<210\,K}}{CCA_{total}} \times 100$$

where CCA total is the total cloud covered area, CCA BT <210K is the cloud covered area with cloud top temperature less than 210 K and CCAP BT <210K is the percentage of the total CCA with cloud top temperature less than 210 K. Similarly,

$$CCAP_{210\,K<BT<240\,K} = \frac{\mathrm{CCA}_{210\mathrm{K}<\mathrm{BT}<240\mathrm{K}}}{\mathrm{CCA}_{total}} \times 100$$

Results and Discussion

TIR brightness temperature images of HUDHUD cyclone

An example of the TC diurnal cycle of the CCA and CTT for cyclone HUDHUD on 10th and 11th Oct. 2014 is shown in Figure 1. The TIR-BT enhanced images of HUDHUD cyclone (Fig. 1) shows that the areal extent of deep cold clouds decreases from 500 km to 300 km during day-time (0600-1800 IST) while it increases rapidly from 300 km to 500 km during night- time (1800-0600 IST). The areal extent of relatively warm clouds increases during day-time but decreases during the night-time. In the case of cyclone HUDHUD, most of the areas of cloud within 200 km radius of the TCs centre were covered with clouds colder than 220 K. The change in the TIR-BT associated with changes in the areal extent of the cloud between morning to evening and evening to morning were as 50-70 ◦C. This cyclone is a clear example of different diurnal variations occurring under two different types of clouds (deep cold cloud and cold cloud).

Variation of cloud cover area and cloud top temperature of specific cyclone

The temporal evolution of the areal extent of the clouds and TIR-BT for the cyclone Hudhud and Vardah during their life cycles, are shown in Fig. 2A and Fig. 2B. It can be noted from the CCA plots that diurnal variation of CCA of deep cold clouds and cold clouds are opposite in phase and magnitude in the inner region of the cyclones. Similar trends are observed for outer region of cold clouds and warm clouds. The diurnal variation of CTT of deep cold clouds and cold clouds are also observed to be opposite in phase but have approximately 3 hrs lag in the inner region. Similar trend is followed in the outer region for cold cloud (< 240 K) and warm cloud (> 240 K). It is quite interesting that the CCA and CTT are out of phase. When the cold cloud area (<240 K) decreases, there is an increase in the area covered by the warm cloud (>240 K) and vice versa. We can observe two peaks for the day for the average temperature of the outer region (300-500 km) by the two leading out-of-phase conditions namely CCA and CTT.

Diurnal variation of mean cloud cover area and mean cloud top temperature

The diurnal variation of the mean CCA and CTT for all the considered cyclones during 24 hours is shown in Figs. 3A, 3B, 4A and 4B. Fig. 3A (Fig. 4A) shows the plots for BoB (ARB) cyclones which formed during 2008-2012 using Kalpana-1 data. We observed that in the inner [Fig. 3A(a) and Fig. 4A(a)] and outer region [Fig. 3A(c) and Fig. 4A(c)] the area covered by deep cold clouds reaches a maximum during morning (0600-0800 IST) and then decreases after sunrise becomes minimum during the evening (1800-2100 IST). Considering the cold clouds, the maximum CCA is found at the afternoon (1200-1400 IST) for the inner region [Fig. 3A(b) and Fig. 4A(b)] and outer region [Fig. 3A(d) and Fig. 4A(d)]. The CTT of deep cold clouds in the inner region [Fig. 3A(a) and Fig. 4A(a)] and outer region [Fig. 3A(c) and Fig. 4A(c)] are maximum during afternoon (1200-1500 IST) but minimum occurs during midnight (24000600 IST). In the case of cold clouds the CTT is found to be maximum during early morning hours in the inner [Fig. 3A(b) and Fig. 4A(b)] and outer region [Fig. 3A(d) and Fig. 4A(d)] of the cyclones. The similar trends and results are found when the INSAT-3D data is used in the calculation of CCA and CTT for the cyclones (2013-2016) and the corresponding plots are shown in Fig. 3B (BoB) and 4B (ARB) respectively.

Diurnal variation of mean cloud top temperature with radial distance from TC centre

From the Fig. 5A, at any given particular time the mean TIR-BT increases with increase in the radial distance from the TC centre. A minimum TIRBT is found at morning (0300-0600 IST) for inner region except 0-100 km and during afternoon (1200-1800 IST) for outer region. Further, it is observed that a minimum TIR-BT for the cold clouds occurs at morning while for the warm clouds occurs at afternoon (1500 IST). In the ARB basin (Fig. 6A) the analysis using the Kalpana data shows that the TIR-BT is minimum during morning hours (0900 IST) for inner region of TC. However, during the evening hours (1800-2400 IST) the minimum TIR-BT occurs for outer region from the TC centre. In the ARB basin the minimum of the cold clouds occur during morning hours while that of warm clouds occur during evening hours with a bias of 1 hour. The analysis with the INSAT-3D data in BoB and ARB basins in presented in Fig. 5B and Fig. 6B respectively. The diurnal variation of the mean CTT observed using INSAT-3D data to be same as the mean CTT observed with the Kalpana1 data, in both the basins. For the outer region (300-500 km) covering the area of mid-level clouds, low level clouds and clear sky are found at late afternoon. The main two causes for the semi-diurnal cycle in the radius-averaged TIR-BT is, one being out-of-phase relationship between TIR-BT conditions (TIR-BT < 240 K or TIR-BT > 240 K) and second under two different cloud conditions (deep cold cloud or cold cloud). In BoB basin clouds with TIR-BT < 210 K has minimum mean temperature from mid-night to early morning (Fig. 5A and 5B), while ARB basin has the minimum mean temperature in the morning (Fig. 6A and 6B).

Diurnal variation of mean cloud coverage area below particular thresholds of TIR-BT

In order to observe, the mean diurnal CCA variability with TIR-BT of 190260 K, the mean areal extent with TIR-BT of 190-260 K is also calculated for various thresholds of TIR-BT within the 500 km radius from the TC centre (Figs. 7A, 7B, 8A and 8B). The data shown in the Fig. 5 and 6 marks that diurnal variability of TC convective systems are also in terms with the CCA and CTT. The analysis with Kalpana data during 2008-2013 in BoB (Fig. 7A) shows that at any given time when the threshold limit is increased then the mean CCA also increases. It is also observed that for the maximum mean CCA of deep cold cloud occurs during morning (0600-0900 IST) and warm cloud occurs during afternoon (1500 IST). Due to inadequate Kalpana satellite data in ARB basin (Fig. 8A) during 2008-2012, no concrete conclusion of 190-260 K can be made. The diurnal variation of mean CCA is observed to be same as observed with the Kalpana-1 data in BoB basins, with the INSAT-3D data in BoB (Fig. 7B) and ARB (Fig. 8B) during 2013-2016.

For BoB basins, the total area covered by the cloud-top is colder than 200, 220 and 260 K, has maximum areal extend at 2400, 0300 and 1500 IST while in the ARB basin the total area covered by cloud-tops colder than 200, 230 and 260 K has maximum areal extent at 0600, 0900 and 1500 IST respectively. This phenomenon indicates that the time at which maximum CCA occurred over the oceans was sensitive to TIRBT threshold used for both BoB and ARB basins. From the previous results (e.g. Strenka *et al.*, 2014), it can be observed that different TIR-BT thresholds causes diurnal cycles in deep convection and cloud patterns in TCs.

Diurnal variations of mean cloud coverage area percentage and mean cloud top temperature

The mean diurnal cycles of the total areas covered by deep cold cloud tops and by cold clouds tops together with their respective mean CCAP and mean CTT are shown in Figs. 9A, 9B, 10A and 10B respectively. We used these results to determine whether the coverage of cloud tops colder than 210 K and clouds tops between 210 K and 240 K were related or developed independently. In both BoB and ARB basins [Fig. 9A(a) and 10A(a)] shows that the mean CCAP of deep cold clouds tops reached a maximum during the morning (0600 IST) which starts decreasing after sunrise and reaches a minimum during evening hours (1800 IST). However, the mean CCAP [Fig. 9A(b) and 10A(b)] of cold cloud tops attain maximum during afternoon hours (1500 IST) and minimum during early morning hours (0300 IST). The mean TIR-BT of deep cold clouds [Fig. 9A(a) and 10A(a)] are maximum occurs during the noon time (1200 IST) and minimum CTT occurs during midnight (0000 IST). The mean TIR-BT of cold cloud [Fig. 9A(b) and 10A(b)], is observed to be maximum during evening hours (1800 IST) and minimum during morning (0600-0900 IST). Similarly, the analysis from the INSAT-3D data in BoB [Fig. 9B(a) and Fig. 9B(b)] during 2013-2016 and ARB during 2008-2012 [Fig. 10B(a) and Fig. 10B(b)] suggests that deep cold cloud coverage (%) is maximum during morning and minimum during evening but the cold cloud coverage (%) is found to be maximum during afternoon and minimum during morning or early morning. The analysis of the mean brightness temperature plots of deep cold cloud temperature shows that it attains maximum during noon and minimum occurs at midnight, while for cold clouds the maximum CTT occurs during evening and minimum during morning respectively. The maximum area of deep cold cloud tops in the morning suggests that deep cold cloud with TIR-BT < 210 K, followed the cloud radiation interaction hypothesis. The decrease in the coverage of deep cold cloud was followed by an increase in coverage of cold cloud. In both BoB and ARB basin storms the mean CCA of deep cold clouds was about half of cold clouds (210 K < TIR-BT < 240 K). The diurnal CTT were out-of-phase with diurnal variation of CCA. The maximum and minimum temperature cold cloud (210-240 K) were about 3 hour later than the maximum and minimum temperatures of the deep cold clouds.

Table 1: Information during day and night time

During day hours	During night hours
More unstable	Less unstable
Convection increases	Convection decreases
Latent heat increases	Latent heat decreases
Rising motion increases	Rising motion decreases
Lapse rate increases	Lapse rate decreases
Surface pressure decreases	Surface pressure increases
Precipitation increases	Precipitation decreases

Figure.1 TIR enhanced brightness temperature showing Hudhud Cyclone (a,b) 0600 IST and 1800 IST 10th Oct. 2014 and (c,d) 0600 and 1800 IST 11 th Oct. 2014

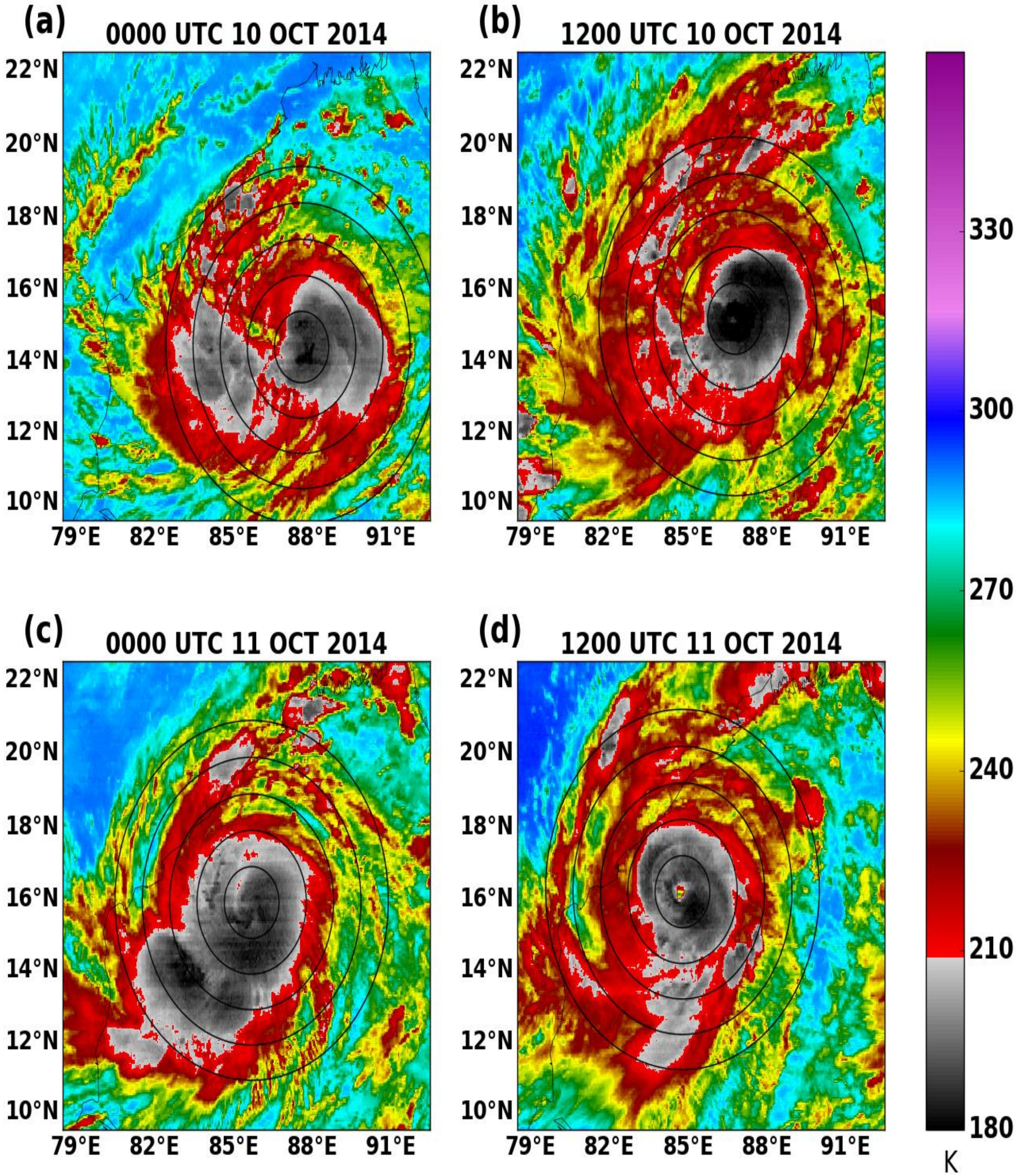

Figure 2: Three-hourly (IST) TIR data of Hudhud and Vardah cyclone for (a) areal extent and (c) radius- averaged TIR-BT at inner region from the TC centre. The red lines show TIR-BT and green lines show TIR-BT lies between 210 to 240 K. Three-hourly (IST) TIR data (b) areal extent and (d) radius averaged TIR-BT at outer region from the TC centre. The red lines show TIR-BT < 240 K and green lines show TIR-BT > 240 K. 8

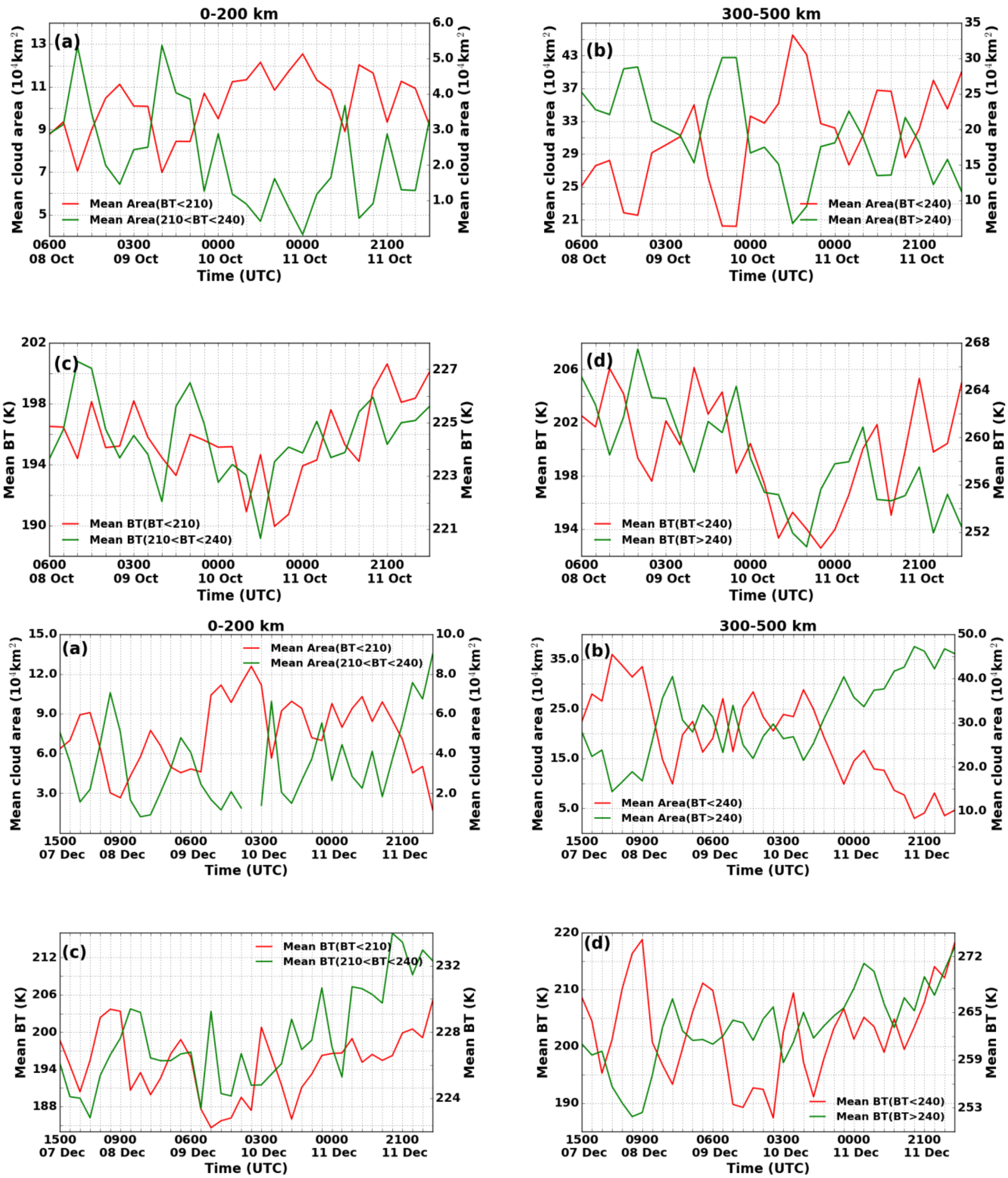

Figure 3: Using Kalpana-1 (2008-2013) and INSAT-3D (2013-2016) satellite TIR-BT data over BoB basins mean diurnal variation of CCA and CTT for (a,c) inner and outer region when CTT < 210 K and for (b,d) inner and outer region when CTT lies between 210 to 240 K. The green lines show mean CCA and red lines shows mean CTT.

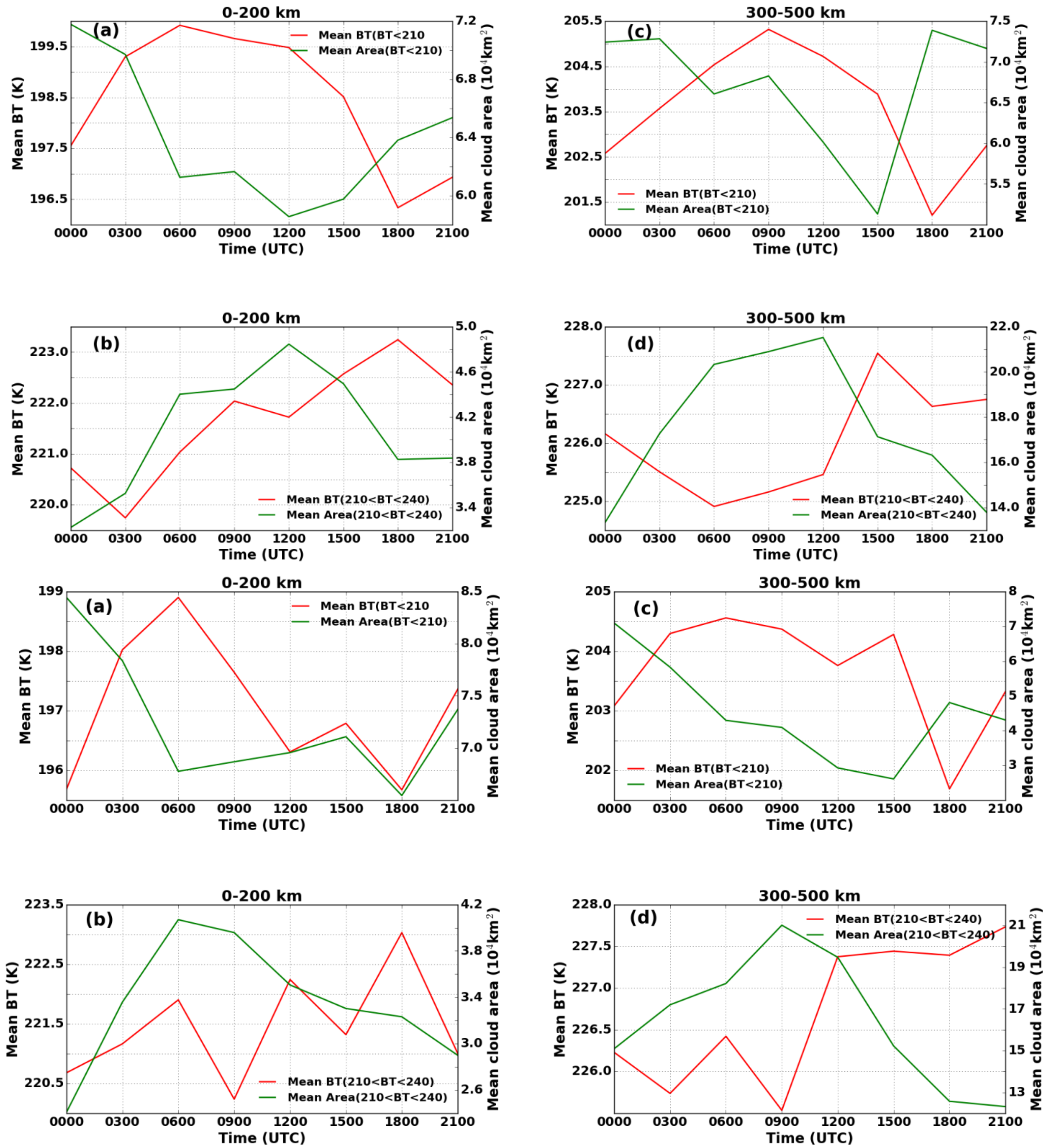

Figure 4: Using Kalpana-1 (2008-2013) and INSAT-3D (2013-2016) satellite TIR-BT data over ARB basins mean diurnal variation of CCA and CTT for (a,c) inner and outer region when CTT < 210 K and for (b,d) inner and outer region when CTT lies between 210 to 240 K. The green lines show mean CCA and red lines shows mean CTT.

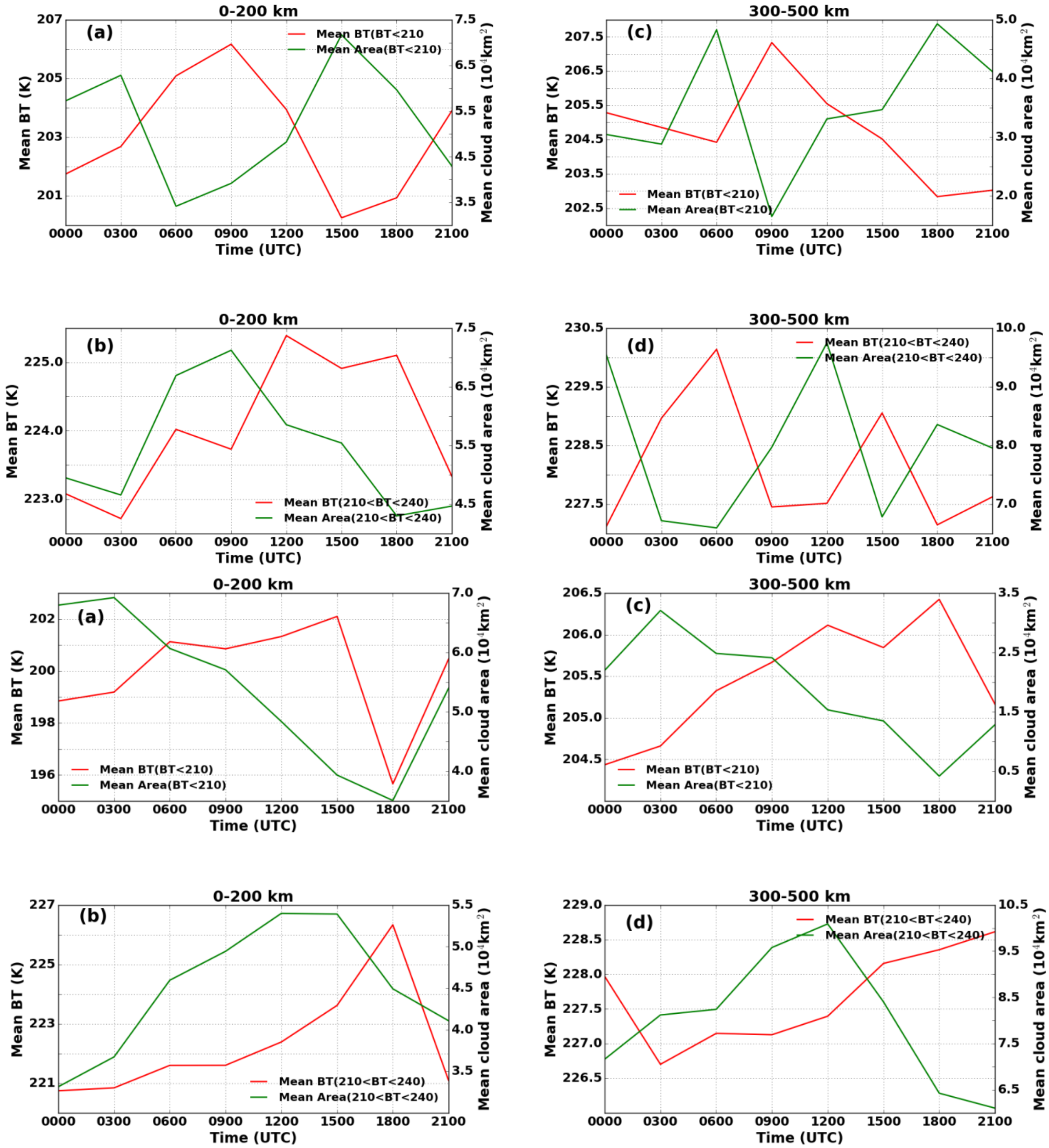

Figure 5: Using Kalpana-1(2008-2012) and INSAT-3D (2013-2016) satellite data in BoB basins, the mean diurnal variation of CTT at 0-50, 50-100, 100-150, 150200, 200-250, 250-300, 300-350, 350-400, 400-450 and 450-500 km annular region from the TC centre.

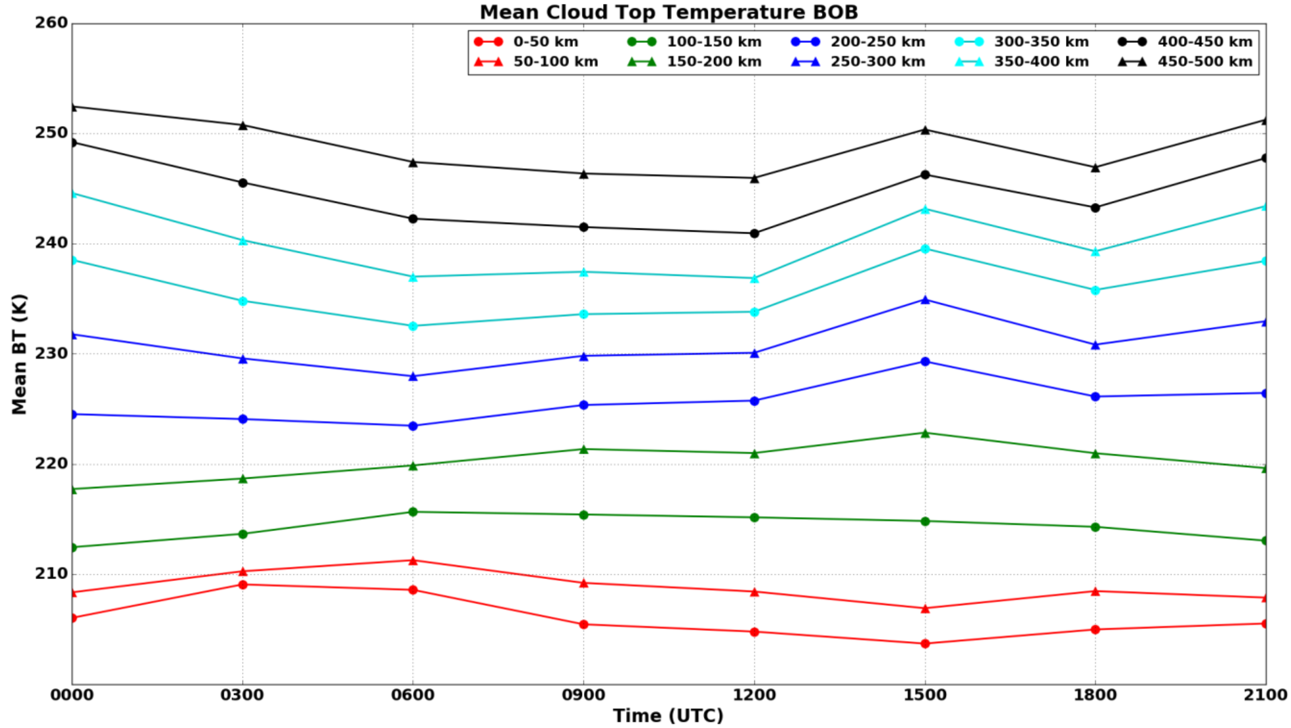

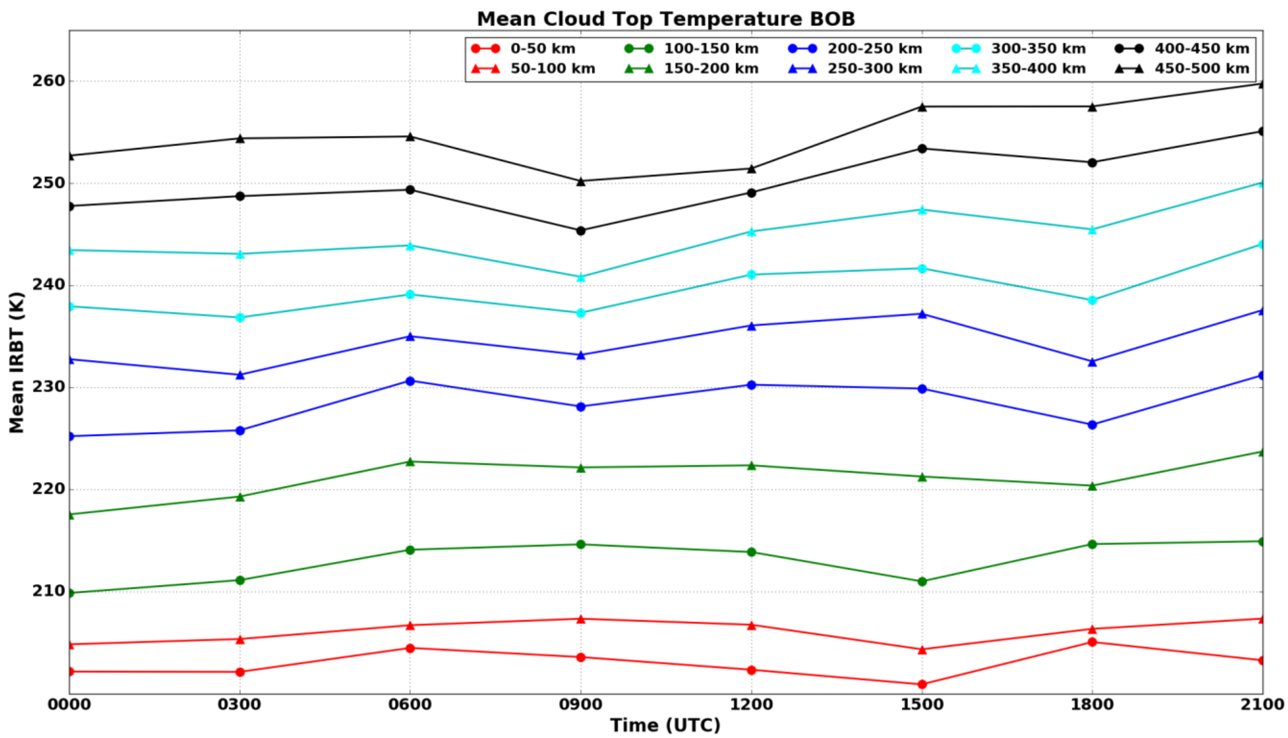

Figure 6: Using Kalpana-1 (2008-2012) and INSAT-3D (2013-2016) satellite data in ARB basins, the mean diurnal variation of CTT at 0-50, 50-100, 100-150, 150200, 200-250, 250-300, 300-350, 350-400, 400-450 and 450-500 km annular region from the TC centre

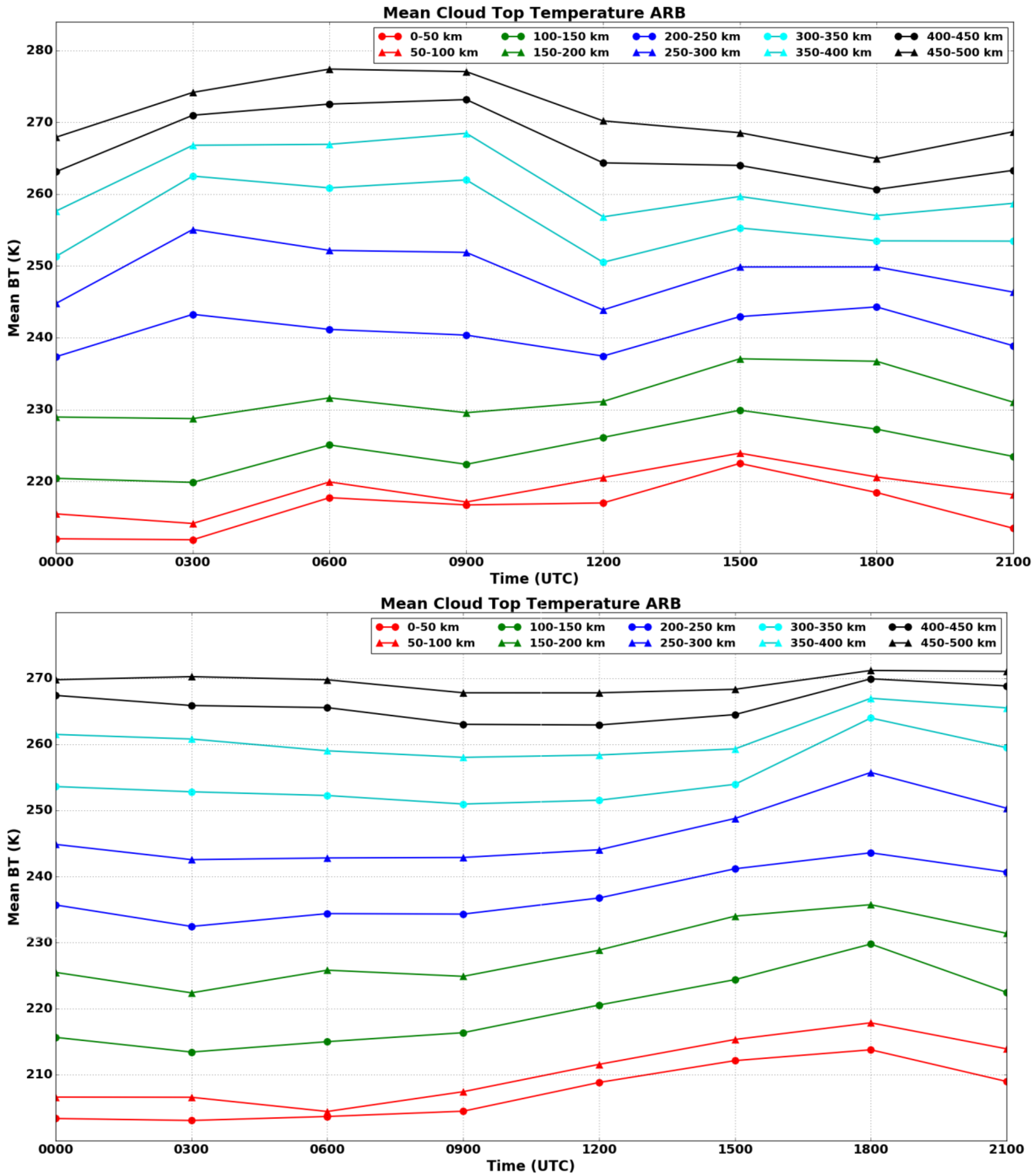

Figure 7: Using Kalpana (2008-2013) and INSAT-3D (2013-2016) satellite data in BoB basins, the mean diurnal variation of CCA when the cloud top TIR-BT < 190 K, < 200 K, < 210 K, < 220 K, < 230 K, < 240 K, < 250 K and < 260 K within 500 km radius from the TC centre. 16

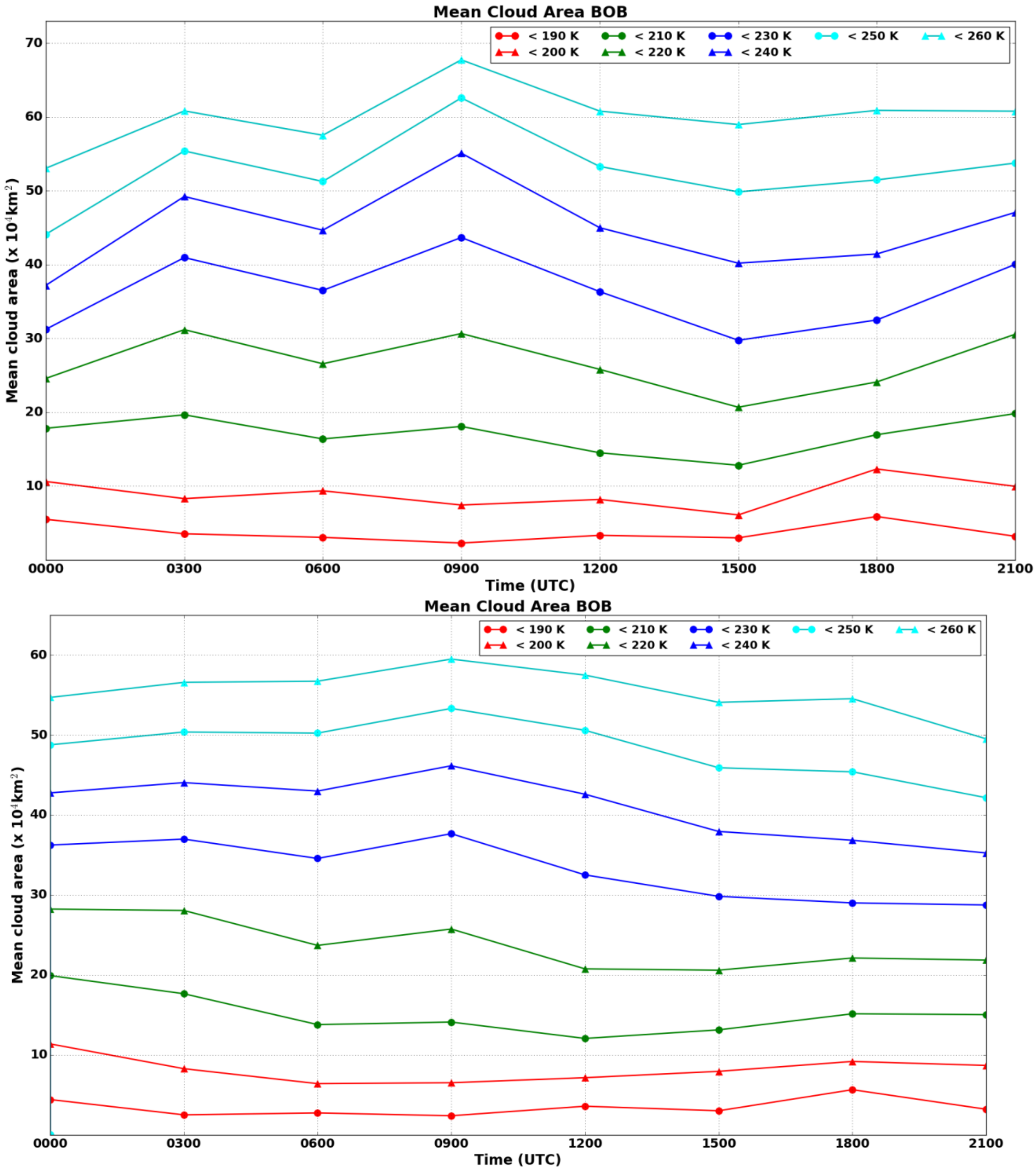

Figure.8 Using Kalpana (2008-2013) and INSAT-3D (2013-2016) satellite data in ARB basins, the mean diurnal variation of CCA when the cloud top TIR-BT < 190 K, < 200 K, < 210 K, < 220 K, < 230 K, < 240 K, < 250 K and < 260 K within 500 km radius from the TC centre

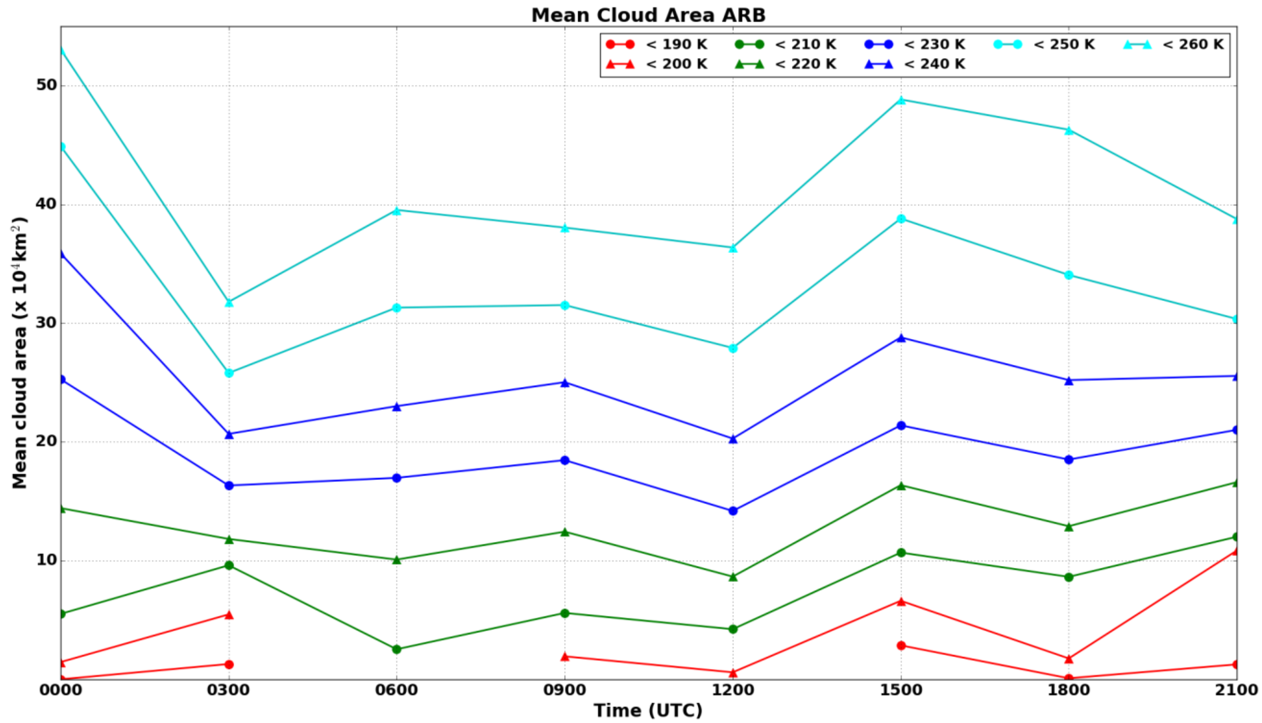

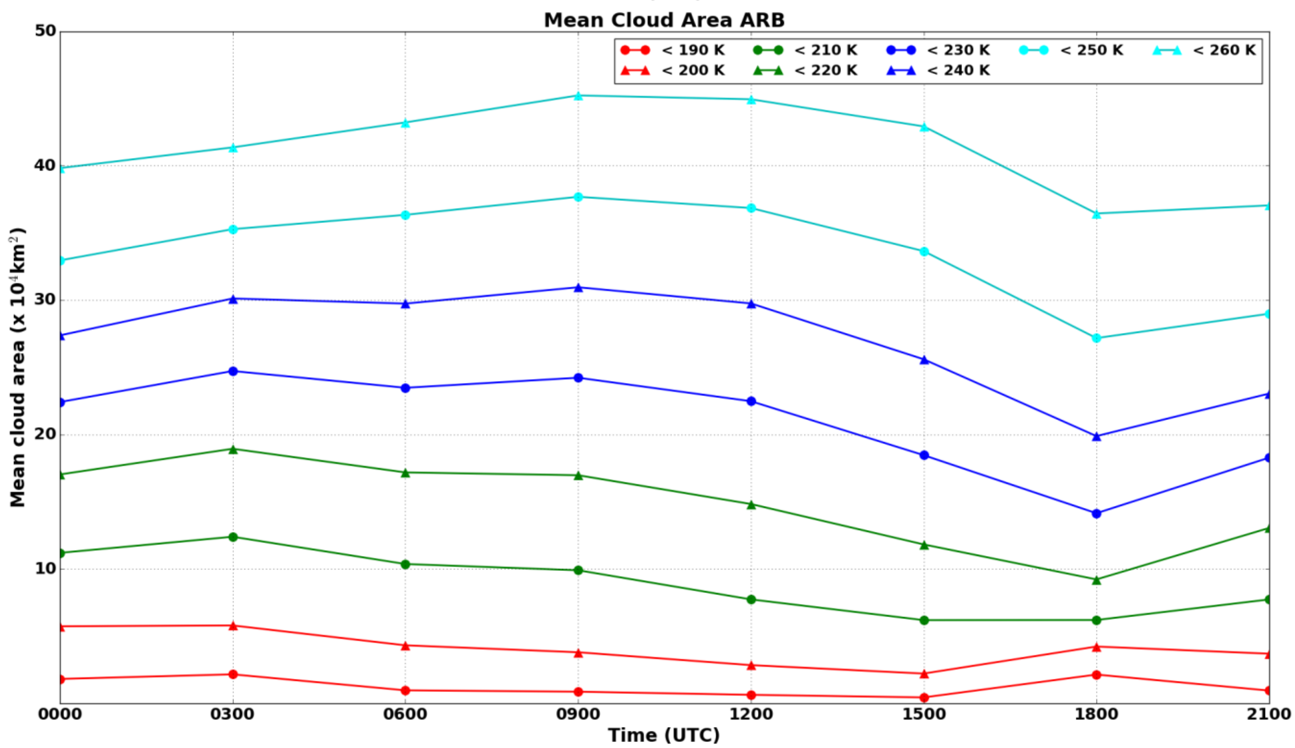

Figure.9 Using Kalpana-1 (2008-2013) and INSAT-3D (2013-2016) satellite data over BoB basins mean diurnal variations in CTT and cloud coverage percentage (percentage to 500 km from the TC centre) for (a) CTT < 210 K and (b) CTT between 210-240 K. The green lines show mean cloud coverage percentage and red lines show mean CTT. 19

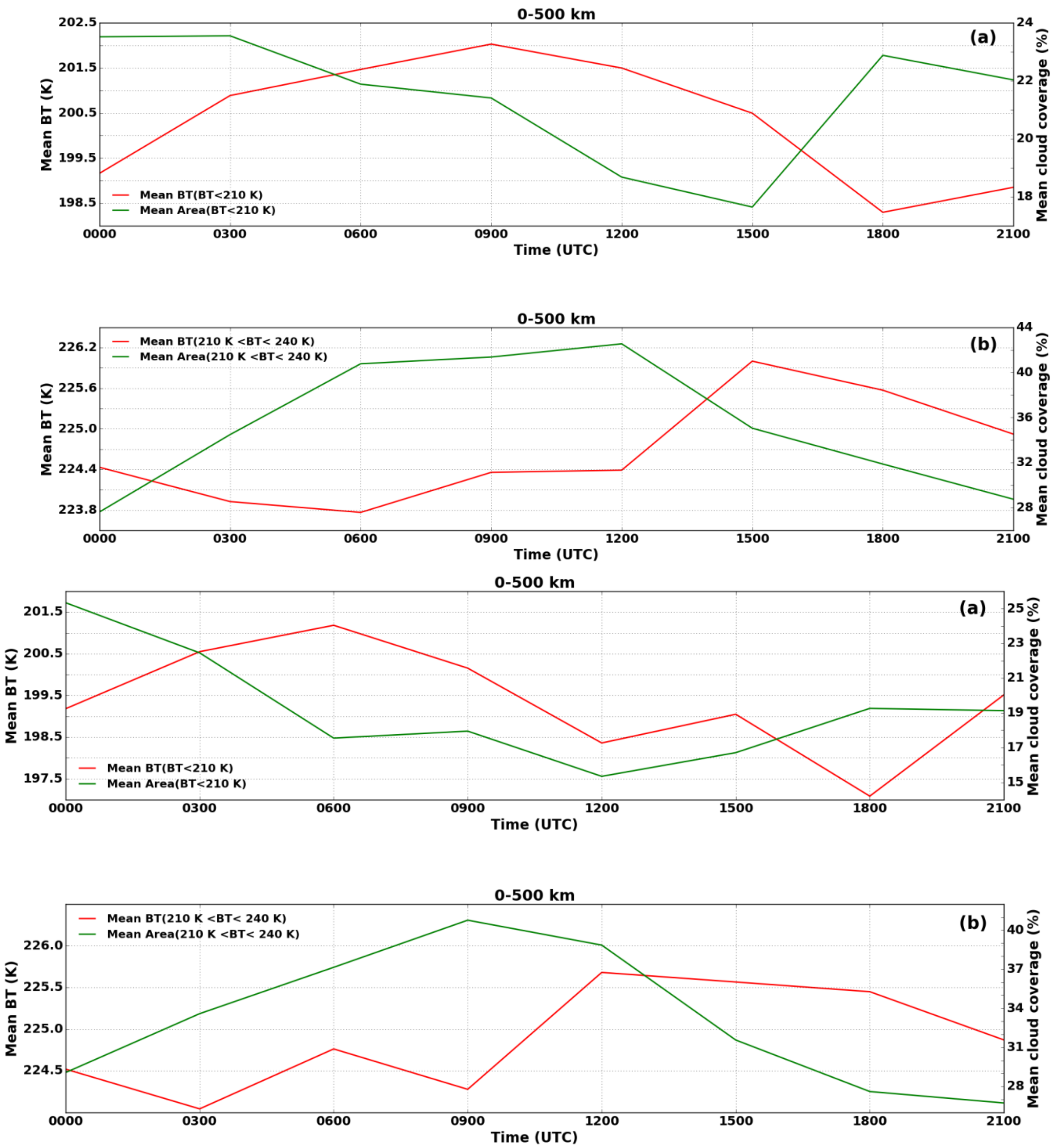

Figure.10 Using Kalpana-1 (2008-2013) and INSAT-3D (2013-2016) satellite data over ARB basins mean diurnal variations in CTT and cloud coverage percentage (percentage to 500 km from the TC centre) for (a) CTT < 210 K and (b) CTT between 210-240 K. The green lines show mean cloud coverage percentage and red lines show mean CTT

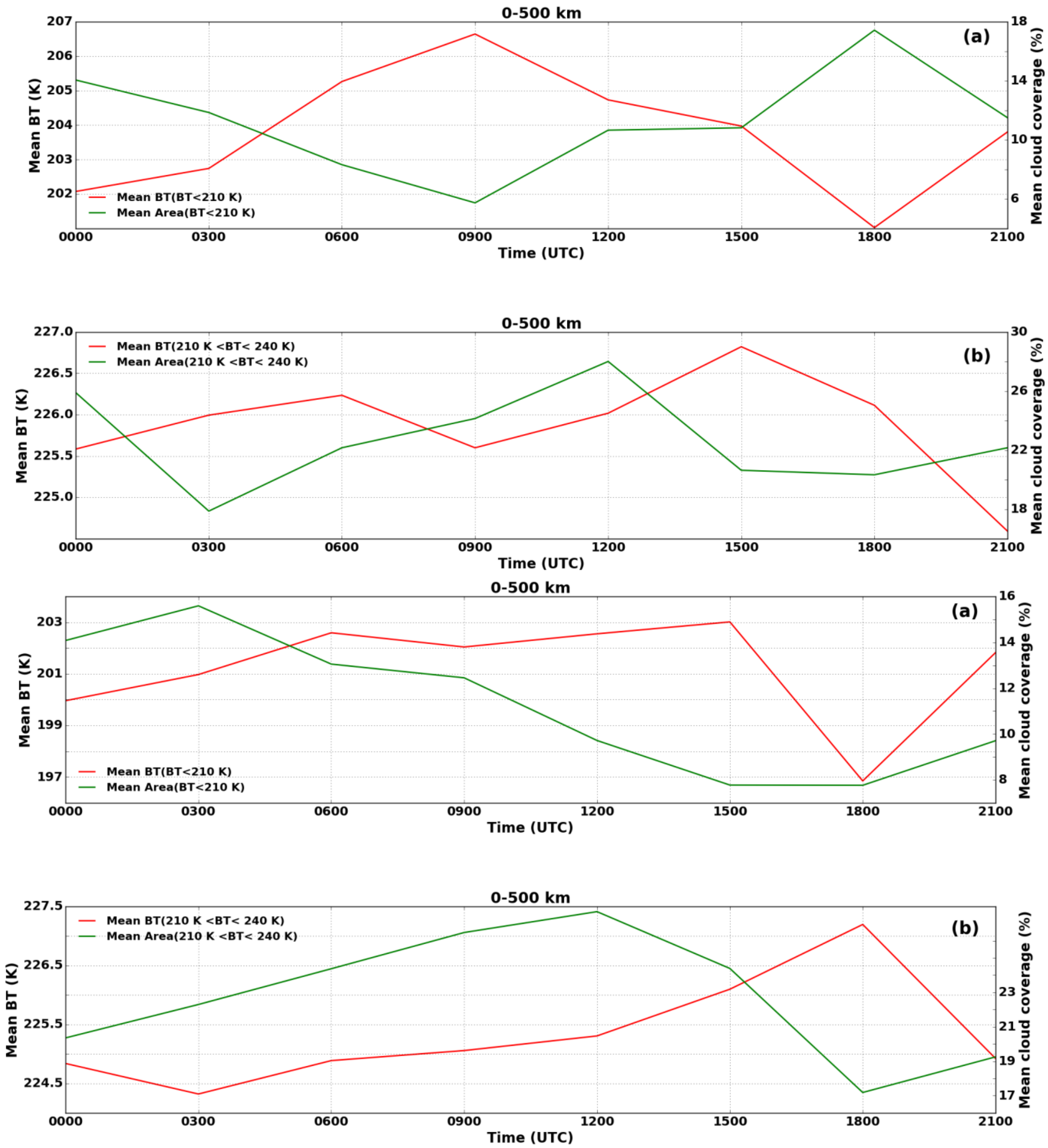

The difference between diurnal pulses in TIR-BT and precipitation in TCs

Wu *et al.,* (2015) and Dunion *et al.,* (2014) found a distinguishing characteristic of the TC is the diurnal pulses and diurnal amplitude of precipitation decreases when radial distance increases from the TC centre. The changes in CTT and CCA is reflected by the two cloud conditions namely TIR-BT cooling and precipitation. The cloud held of HUDHUD cyclone cooled by 50-70˚C 200-300 km from TC centre during night (Fig. 1). This was achieved through the deep cold cloud extending from 200 to 300 km from TC centre. From the TC centre to a particular distance the solely TIR-BT changes cannot predict the diurnal cycles of TC. So, CTT and time at which CCA occurs describes the diurnal cycles better.

Mechanisms involved in two types of diurnal variation of cloud

The present study results suggest that the maximum occurrence of deep cold clouds in the morning can be explained using hypothesis based cloud radiation interactions. According to Chen and Houze (1997) the maximum occurrence of cold cloud in the afternoon followed the diurnal solar heating of the ocean surface and atmospheric boundary layer. So the cause of diurnal variation of areas, clouds top temperature can be explained by the following conceptual models (Hobgood, 1986). As per the conceptual model, the diurnal cycle of net radiation at the cloud tops are identified as the primary causes of the oscillation. Radiative cooling of the cloud tops at night steepens the lapse rate which in turns increases convection. This generates a slight intensification in the storm, the reverse occurs during the day time, as the cloud tops absorb solar radiation and the absorption of solar radiation during the day creates slightly warmer conditions at the cloud tops consequently increasing the stability. During night, lower temperature causes a decrease in the stability. The conceptual model is summarised in Table 1.

And cloud radiation and interaction during day and night are shown in Fig. 4.51. The changes in stability generate increased convection at night produced more precipitation, greater latent heating, more rising motion and slightly lower surface pressures. The decreased convection during the day generates less precipitation; reduce latent heating, less rising motion and higher pressures. In addition, the changes in convection affect the development at the cirrus canopy and its areal extent. As the storm develops and the radiative fluxes become a smaller proportion of the total energy budget, the diurnal fluctuations becomes less pronounced. The cirrus clouds are connected to deep convective cloud as cirrus cloud are at high heights. So cirrus cloud can explain the phase difference between TIR-BT < 210 K and 210 K < TIR-BT < 240 K over the ocean. The outwards propagation of the diurnal signals from the TC centre appears to be related to the internal structure of the TC convective systems in NIO basins (Wang, 2009). Chan and Williams (1987); Yang and Slingo (2001) speculated that gravity waves emanating from the diurnally driven land convective systems were responsible for an identical diurnal signal over adjacent oceans. In another examples, the propagation of the diurnal signals from the convective systems associated with the Madden-Julian Oscillation was considered to be related to the unique land- sea distribution of Maritime continent (Ichikawa and Yasunari, 2007; Julian and Madden, 1981). In this study of Mapes *et al.,* (2003), the diurnally driven gravity waves from convection in the Northwestern South America were found to have a propagation speed of 15 m/s. Given that these studies all identify a similar mechanism for the propagation of diurnal signals; we speculate that the propagation observed in TCs, in this study is also caused by diurnal driven gravity waves with a speed of 10-20 m/s. The rain bands propagate outwards from the TC centre in a manner similar to the TC inner core and outer rain bands are different. Whether the inner core and the outer rain bands responds differently to the diurnal radiative forcing or the diurnal signals propagates from the inner core outwards to the outer rain bands is worth exploration.

Concluding remarks

The diurnal variations of the CCA, and CTT in deep cold cloud, cold cloud and warm cloud system in TCs over the NIO basins were analysed using pixel resolution of TIR-BT data and best-track data from 2008 to 2016 which included a total of 31 cyclones. The diurnal variations of these TCs of convective systems could be described as precisely as possible. During this analysis the CCA of deep cold cloud decreases during the day time while increases during the night time, but the variation is opposite in the case of cold clouds. The variation of CCA and CTT of deep cold and cold cloud are opposite in phase and magnitude for inner region of TCs. Similar trends are also found in outer region of TCs for cold and warm cloud. But in the case of CTT 3-hr lag is observed. If CTT are maximum then CCA are minimum at a particular time. The diurnal variation of mean CCA of deep cold clouds are maximum during morning while the mean CCA of cold clouds are maximum at afternoon for inner and outer region of TCs. The cold cloud had minimum mean CTT during the morning while warm cloud had minimum mean CTT during the afternoon for inner and outer region of TCs. The out-of-phase relationship between the areal extents under these different types of cloud led to substantial variations in the time at which the maximum of cold cloud occurred, depending on the TIR-BT thresholds used. At a particular time, the deep cold cloud areas are maximum then the cold cloud area are minimum. At a particular time, the mean CTT increases with increasing in the radial distance from the TC centre and at any particular time when the threshold limit are increased then the mean CCA increases. The mean CTT of TIR-BT < 220 K are minimum occurs during morning for inner region while the mean CTT of TIR-BT > 230 K are minimum evening for the outer region. The mean CCAP of deep cold cloud top reaches a maximum during the morning which starts decreasing after sunrise and reaches a minimum during evening. The mean CCAP of cold cloud are maximum during the afternoon and minimum during evening. The mean CTT of deep cold clouds are minimum during the midnight while the cold cloud top temperature occurs during the morning. The diurnal cycles in TC convective cloud systems are complicated by diurnal variation in the horizontal size of clouds and by cloud temperature having different phases under different conditions. Hypothesis for cloud-radiation interaction have been developed to explain day time minima and night time maxima in cloud cover.

Acknowledgements

The authors would like to acknowledge to Dr. Satya Prakash Ojha and Dr. V. Satyamoorthy Indian Satellite Research Organisation, and Dr. C. Shaji, Indian Institute of Technology Kharagpur for their helpful suggestions and variable comments. The TC track data obtained from the IMD (www.rsmcnewdelhi.imd.gov.in). TIR-BT data were obtained the MOSDAC (www.mosdac.gov.in).

References

Biondi, R., Ho, S. P., Randel, W., Syndergaard, S., and Neubert, T. (2013). Tropical cyclone cloud-top height and vertical temperature structure detection using GPS radio occultation measurements. Journal of

Geophysical Research: Atmospheres, 118(11), 5247-5259.
Bowman, K. P., and Fowler, M. D. (2015). The diurnal cycle of precipitation in tropical cyclones. Journal of Climate, 28(13), 5325-5334.
Browner, S. P., Woodley, W. L., and Grith, C. G. (1977). Diurnal oscillation of the area of cloudiness associated with tropical storms. Monthly Weather Review, 105(7), 856-864.
Chan, J. C., and Williams, R. T. (1987). Analytical and numerical studies of the beta-eect in tropical cyclone motion. Part I: Zero mean ow. Journal of the atmospheric sciences, 44(9), 1257-1265.
Chan, J. C., and Williams, R. T. (1987). Analytical and numerical studies of the beta-eect in tropical cyclone motion. Part I: Zero mean ow. Journal of the atmospheric sciences, 44(9), 1257-1265.
Chen, S. S., and Houze, R. A. (1997). Diurnal variation and life-cycle of deep convective systems over the tropical Pacic warm pool. Quarterly Journal of the Royal Meteorological Society, 123(538), 357-388.
Clark, J., and Chu, P. S. (2002). Interannual variation of tropical cyclone activity over the central North Pacic. Journal of the Meteorological Society of Japan. Ser. II, 80(3), 403-418.
Dunion, J. P., Thorncroft, C. D., and Velden, C. S. (2014). The tropical cyclone diurnal cycle of mature hurricanes. Monthly Weather Review, 142(10), 3900-3919.
Emanuel, K. A. (1989). The nite-amplitude nature of tropical cyclogenesis. Journal of the Atmospheric Sciences, 46(22), 3431-3456.
Fiorino, M., and Elsberry, R. L. (1989). Contributions to tropical cyclone motion by small, medium and large scales in the initial vortex. Monthly weather review, 117(4), 721-727.
Frank, W. M. (1977). The structure and energetics of the tropical cyclone II. Dynamics and energetics. Monthly Weather Review, 105(9), 1136-1150.
Gray, W. M. (1975). Tropical cyclone genesis. Atmospheric science paper; no. 234.
Gray, W. M. (1981). Recent advances in tropical cyclone research from rawinsonde composite analysis. WMO.
Gray, W. M., and Jacobson Jr, R. W. (1977). Diurnal variation of deep cumulus convection. Monthly Weather Review, 105(9), 1171-1188.
Harr, P. A., Kalafsky, M. S., and Elsberry, R. L. (1996). Environmental conditions prior to formation of a midget tropical cyclone during TCM-93. Monthly weather review, 124(8), 1693-1710.
Hobgood, J. S. (1986). A possible mechanism for the diurnal oscillations of tropical cyclones. Journal of the atmospheric sciences, 43(23), 2901-2922.
Holton, J. R., and Hakim, G. J. (2012). An introduction to dynamic meteorology (Vol. 88). Academic press.
Hong, G., Heygster, G., and Rodriguez, C. A. M. (2006). Eect of cirrus clouds on the diurnal cycle of tropical deep convective clouds. Journal of Geophysical Research: Atmospheres, 111(D6).
Ichikawa, H., and Yasunari, T. (2007). Propagating diurnal disturbances embedded in the Madden-Julian Oscillation. Geophysical Research Letters, 34(18).
Janowiak, J. E., Arkin, P. A., and Morrissey, M. (1994). An examination of the diurnal cycle in oceanic tropical rainfall using satellite and in situ data.

Monthly weather review, 122(10), 2296-2311.

Kieper, M. E., and Jiang, H. (2012). Predicting tropical cyclone rapid intensification using the 37 GHz ring pattern identified from passive microwave measurements. Geophysical Research Letters, 39(13).

Liu, L., Zheng, J., Ruan, Z., Cui, Z., Hu, Z., Wu, S., ... and Wu, Y. (2015). Comprehensive radar observations of clouds and precipitation over the Tibetan Plateau and preliminary analysis of cloud properties. Journal of Meteorological Research, 29(4), 546-561.

Madden, R. A., and Julian, P. R. (1994). Observations of the 4050-day tropical oscillation A review. Monthly Weather Review, 122(5), 814-837.

Maloney, E. D., and Hartmann, D. L. (2001). The Madden Julian oscillation, barotropic dynamics, and North Pacic tropical cyclone formation. Part I: Observations. Journal of the atmospheric sciences, 58(17), 2545-2558.

Mapes, B. E., Warner, T. T., Xu, M., and Negri, A. J. (2003). Diurnal patterns of rainfall in Northwestern South America. Part I: Observations and context. Monthly Weather Review, 131(5), 799-812.

Muramatsu, T. (1983). Diurnal variations of satellite-measured TBB areal distribution and eye diameter of mature typhoons. Journal of the Meteorological Society of Japan. Ser. II, 61(1), 77-90.

Nesbitt, S. W., and Zipser, E. J. (2003). The diurnal cycle of rainfall and convective intensity according to three years of TRMM measurements. Journal of Climate, 16(10), 1456-1475.

Palm, E. (1959). On the maintenance of kinetic energy in the atmosphere. In The Atmosphere and Sea in Motion (The Rossby Memorial Volume) (pp. 212-224). Rockefeller Inst. Pross New York.

Prat, O. P., and Nelson, B. R. (2013). Precipitation contribution of tropical cyclones in the southeastern United States from 1998 to 2009 using TRMM satellite data. Journal of Climate, 26(3), 1047-1062.

Randall, D. M., and Fernandes, M. F. (1991). The social desirability response bias in ethics research. Journal of business ethics, 10(11), 805-817.

Rao, G. V., and Macarthur, P. D. (1994). The SSM/I estimated rainfall amounts of tropical cyclones and their potential in predicting the cyclone intensity changes. Monthly weather review, 122(7), 1568-1574.

Sato, T., Miura, H., Satoh, M., Takayabu, Y. N., and Wang, Y. (2009). Diurnal cycle of precipitation in the tropics simulated in a global cloud resolving model. Journal of Climate, 22(18), 4809-4826.

Steranka, J., Rodgers, E. B., and Gentry, R. C. (1984). The Diurnal Variation of Atlantic Ocean Tropical Cyclone aloud Distribution Inferred from Geostationary Satellite Infrared Measurements. Monthly weather review, 112(11), 2338-2344.

Steranka, J., Rodgers, E. B., and Gentry, R. C. (1986). The relationship between satellite measured convective bursts and tropical cyclone intensification. Monthly weather review, 114(8), 1539-1546.

Sui, C. H., Lau, K. M., Takayabu, Y. N., and Short, D. A. (1997). Diurnal variations in tropical oceanic cumulus convection during TOGA COARE. Journal of the atmospheric sciences, 54(5), 639-655.

Tian, B., Soden, B. J., and Wu, X. (2004). Diurnal cycle of convection, clouds, and water vapor in the tropical upper troposphere: Satellites versus a general circulation model. Journal of Geophysical Research: Atmospheres, 109(D10).

Trenberth, K. E., Dai, A., Rasmussen, R. M., and Parsons, D. B. (2003). The changing character of precipitation. Bulletin of the American Meteorological Society, 84(9), 1205-1217.

Wu, Q., Ruan, Z., Chen, D., and Lian, T. (2015). Diurnal variations of tropical cyclone precipitation in the inner and outer rainbands. Journal of Geophysical Research: Atmospheres, 120(1), 1-11.

Yang, G. Y., and Slingo, J. (2001). The diurnal cycle in the tropics. Monthly Weather Review, 129(4), 784-801.